



OPEN

Experience of virtual commissioning of a process control system for the production of high-paraffin oil

Yury V. Ilyushin¹✉ & Vadim Fetisov²✉

This work describes the experience in developing and testing software for oil industry automation control systems based on the simulation of technological processes and control systems combined in virtual reality, this approach is called virtual commissioning and is widely used in the world both to create automated process control systems and to simulate interactions between different systems.

The twenty-first century can be described as the century of scientific and technological progress. The growth of industrial production requires a significant increase in the amount of raw materials consumed.

The huge increase in the production of paraffinic and heavy crude oil due to the constant depletion of conventional oil reserves has attracted considerable attention from researchers. The production of waxy deposits in significant quantities can interfere with the flow ability of these waxy crude oils, which can eventually lead to production shut-downs^{1,2}. The deposition and transformation of paraffin molecules into a paraffin gel, which occupies the cross-sectional area of the inner surface of the pipeline, occurs when the bulk oil temperature drops below the paraffin appearance temperature^{3,4}. As a result of the accumulation of paraffin on the walls of the pipeline, the area of oil flow decreases. This phenomenon can lead to an emergency situation and a complete cessation of oil transportation through the pipeline⁵, which can lead to undesirable consequences of stopping production and large economic losses^{6–8}. There are such consequences as the accumulation of paraffin deposits in a large amount, leading to the formation of a paraffin gel^{9,10}, and resulting in aggregation of paraffin in the oil^{11,12} with changes in temperature and pressure; gelation of the paraffin layer, which mainly affects the poor flow ability of waxy crude oils^{13,14}; layered deposition of wax, which leads to blockage of the flow line^{15,16} and which ultimately leads to a complete stop of production processes.

When paraffin is deposited in a pipeline, such mechanisms of molecular diffusion occur¹⁷ as the formation of paraffin crystal nuclei, Brownian motion, and diffusion shift¹⁸. When using a pour point depressant, such phenomena as eutectic adsorption occurs¹⁹. For example, in work²⁰, the authors describe an experiment in which a polarizing microscope was used to observe the morphological lattice of paraffin crystals. In work²¹, the authors conducted an experiment in which wax crystals were formed and separated into three stages using a rheometer that was used when changes in the morphological state of oil occur, as a result of which a change in its viscosity occurs and it is necessary to carry out a physicochemical analysis. For this purpose such laboratory instruments as a gas chromatograph and an infrared spectrometer and other technical methods for determining the quality and composition of oil are used, including both physical and chemical methods^{22–24}.

As an example, which is presented in most of the literature, this is a method for removing paraffin from the pipe walls using scrapers²⁵; this performs the function of the mechanical friction of the scraper against the pipeline wall, as well as heating the pipe cavity^{26,27}. When using pipeline heating, heating detectors and cables are installed on the oil heating pipeline, while the temperature of the heating cable or detector must be higher than the paraffin precipitation temperature^{28,29}. Although it is widely used in oil fields^{30–32}, the heating furnace has a large heat loss, which is not beneficial from either an economic³³ or environmental point of view³⁴. Physicochemical methods³⁵ use the addition of some inhibitors to oil to prevent the formation of paraffin deposits^{36,37}. These inhibitors and depressants improve the rheological properties of crude oil during pipeline transport^{38–40}. Physicochemical methods³⁵ use the addition of certain inhibitors to oil to prevent the formation of paraffin deposits^{36,37}; these inhibitors and pour point depressants^{38–40} such as comb polymers, polyvinyl acetate, amorphous polymers, surfactants and nanohybrids, improve the rheological properties of crude oil in pipeline transport^{41–43}. These

¹Department of System Analysis and Management, Saint Petersburg Mining University, Saint Petersburg, Russia. ²Department of Petroleum Engineering, Saint Petersburg Mining University, Saint Petersburg, Russia. ✉email: ilyushin_yuv@pers.spmi.ru; Fetisov_V@pers.spmi.ru

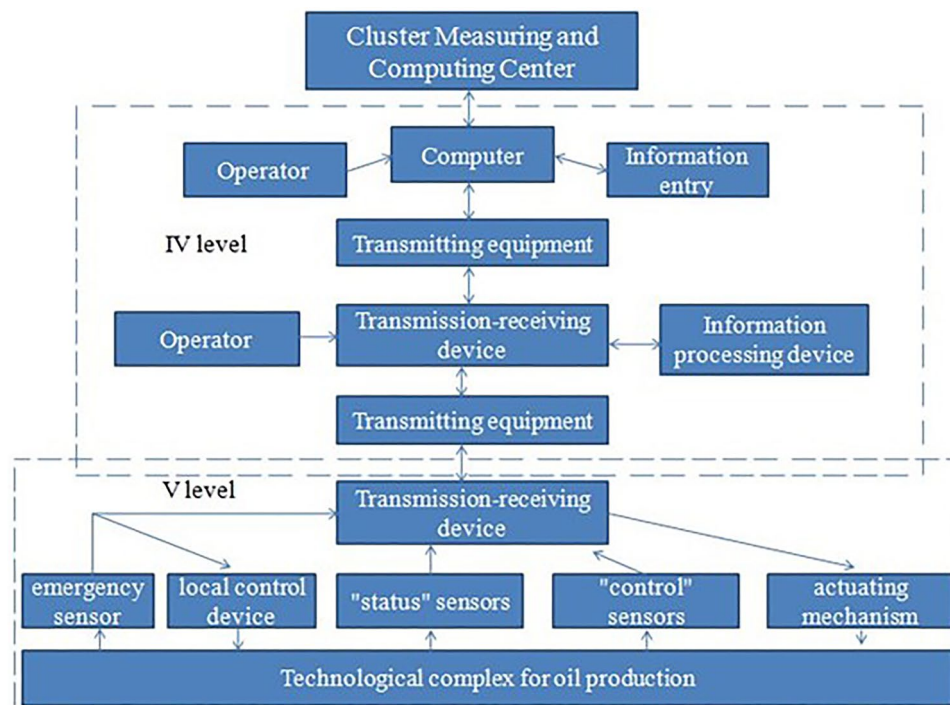


Figure 1. Scheme of information flows in the oil and gas production department in terms of technological complexes for oil production.

paraffins are a mixture of alkanes^{44–46}, which consist of straight and branched chains^{47,48}, solid or liquid state^{49,50}. These include microcrystalline paraffin deposits⁵¹ with a carbon chain from C₁₆ to C₄₀ (alkenyl radicals), as well as isoparaffin hydrocarbons, the content of which is from C₃₀ to C₆₀^{52,53} and which crystallizes into the amorphous structure of the naphthenic ring.

The main tasks aimed at improving the economic efficiency of oil production are the study of linear automatic oil production systems, the construction of their optimal structures, the search for methods and control algorithms⁵⁴, and the patterns of optimal functioning of the technological process.

The purpose of this work is to develop a control system for the process of pulsed heating of a high-paraffin oil flow in the tubing of low-rate oil wells, aimed at reducing the cost of oil production by preventing the formation of asphalt, tar, and paraffin deposits.

Methodology

Existing solution method. Analyzing the oil field as an object of management, it is possible to identify a five-level structure of information interaction in the oil field, which has three administrative levels and two operational levels⁵⁵. The cluster measuring and computing center, which is at the head of the operational level, supplies the central engineering service in real time with operational information about the technical condition and modes of operation of the exploited field, Fig. 1. In the process of applying actions to remove Asphalt-resinous and paraffin deposits in this information scheme, nothing changes, since the technological process for removing Asphalt-resinous and paraffin deposits is not part of the general technological process, but is a third-party, one-time procedure. We will carry out a deep modernization of the technological process by integrating means preventing the formation of Asphalt-resinous and paraffin deposits into the technological process.

Thus, the fifth level of the conceptual model will take the form shown in Fig. 2.

The solution to the key element of this upgrade is the introduction of a pulsed heating element into the system. With this element, the classical mathematical model of the tubing has the form:

$$\frac{\partial T}{\partial t} = a^2 \left(\frac{\partial^2 T}{\partial x^2} + \frac{\partial^2 T}{\partial y^2} + \frac{\partial^2 T}{\partial z^2} \right); \quad (1)$$

$$0 < x < l_x; \quad 0 < y < l_y; \quad 0 < z < l_z.$$

$$T(x, y, L_z \tau) = U(x, y, \tau); \quad \frac{\partial T(x, y, 0, \tau)}{\partial z} = 0; \quad (2)$$

$$T(x, 0, z, \tau) = T(x, l_y, z, \tau) = T(0, y, z, \tau) = T(l_x, y, z, \tau) = 0;$$

$$T(x, y, z, 0) = 0.$$

The equation can be represented as a Green's function.

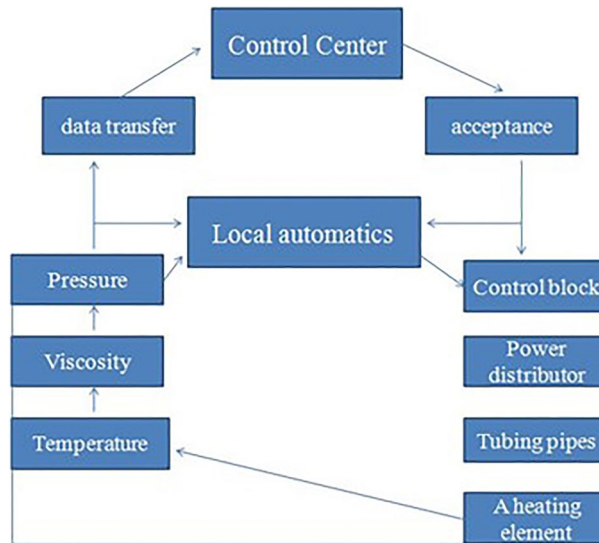


Figure 2. Scheme of information flows of an oil well with installed heating elements.

Mathematical model development. We will obtain dynamic mathematical models to describe the temperature field of oil flow in tubing.

A one-dimensional equation is presented:

$$T(x_j, t) = \sum_{i=1}^d \sum_{n=1}^k \frac{2}{l} \exp \left[-\left(\frac{\pi n a}{l} \right)^2 t \right] \sin \frac{\pi n}{l} x_j \sin \frac{\pi n}{l} \xi_i + \sum_p \sum_{n=1}^k \frac{2}{l} \exp \left[-\left(\frac{\pi n a}{l} \right)^2 (t - \tau_p) \right] \sin \frac{\pi n}{l} x_j \sin \frac{\pi n}{l} \xi_{z(p)}. \tag{3}$$

Two-dimensional equation:

$$T(x_j, y_j, t) = \sum_{i=1}^d \sum_{k,m=1}^{\infty} \frac{4}{l_1 \cdot l_2} \exp \left[-a^2 \pi^2 \cdot t \cdot \left(\frac{k^2}{l_1^2} + \frac{m^2}{l_2^2} \right) \right] \cdot \sin \left(\frac{k \cdot \pi \cdot x_j}{l_1} \right) \cdot \sin \left(\frac{k \cdot \pi \cdot \rho_i}{l_1} \right) \times \sin \left(\frac{m \cdot \pi \cdot y_j}{l_2} \right) \cdot \sin \left(\frac{m \cdot \pi \cdot v_i}{l_2} \right) + \sum_p \sum_{k,m=1}^{\infty} \frac{4}{l_1 \cdot l_2} \cdot \exp \left[-a^2 \pi^2 \cdot (t - \tau_p) \cdot \left(\frac{k^2}{l_1^2} + \frac{m^2}{l_2^2} \right) \right] \times \sin \left(\frac{m \cdot \pi \cdot y_j}{l_2} \right) \cdot \sin \left(\frac{k \cdot \pi \cdot x_j}{l_1} \right) \cdot \sin \left(\frac{k \cdot \pi \cdot \rho_{z(p)}}{l_1} \right) \cdot \sin \left(\frac{m \cdot \pi \cdot v_{z(p)}}{l_2} \right). \tag{4}$$

Equation of a Line in Three Dimensions

$$G(x, y, z, \rho, v, \vartheta, t) = \frac{8}{l_1 \cdot l_2 \cdot l_3} \cdot \sum_{k,m,n=1}^{\infty} B_{k,m,n}(\cdot) \cdot \exp \left[-a^2 \pi^2 \cdot t \cdot \left(\frac{k^2}{l_1^2} + \frac{m^2}{l_2^2} + \frac{n^2}{l_3^2} \right) \right] \tag{5}$$

$$B_{k,m,n}(\cdot) = \sin \left(\frac{k \cdot \pi \cdot x}{l_1} \right) \cdot \sin \left(\frac{m \cdot \pi \cdot y}{l_2} \right) \cdot \sin \left(\frac{m \cdot \pi \cdot z}{l_3} \right) \cdot \sin \left(\frac{k \cdot \pi \cdot \rho}{l_1} \right) \cdot \sin \left(\frac{k \cdot \pi \cdot v}{l_2} \right) \cdot \sin \left(\frac{n \cdot \pi \cdot \vartheta}{l_3} \right). \tag{6}$$

The dependences obtained allow us to carry out numerical simulation of the behavior of the temperature field in time^{55,56}. For a one-dimensional equation, the graph of the dynamic change in the temperature field depending on the number of heating elements should look like the one shown in Fig. 3.

At the Fig. 3 shows the formed temperature field T_1 and T_2 , which is significantly higher than the specified temperature regime. And the greater the number of heating elements d , the higher the temperature field.

Simulation method. In this work, programming in the DELPHI environment was used for a two-dimensional object for controlling the temperature field of oil flow between paraffin molecules in tubing. The graph of the function is shown in Fig. 4a-c.

Figure 4 shows that the generated temperature field has a cyclic nature, and the obtained control algorithms do not use all the heating elements located on the control object⁵⁶. This Figure was made according to the developed mathematical model based on the Green's function which allows you to create a point temperature effect

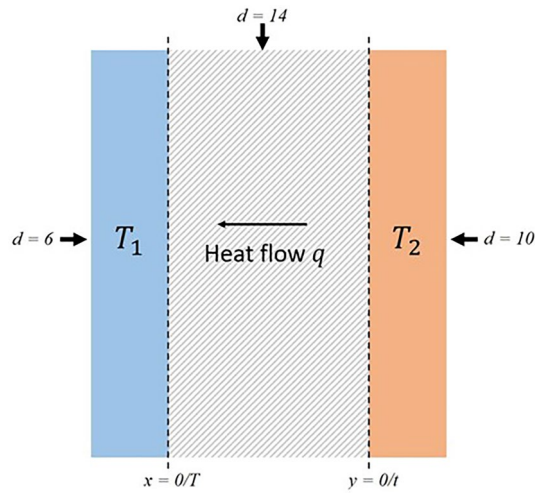


Figure 3. Temperature field values depending on time.

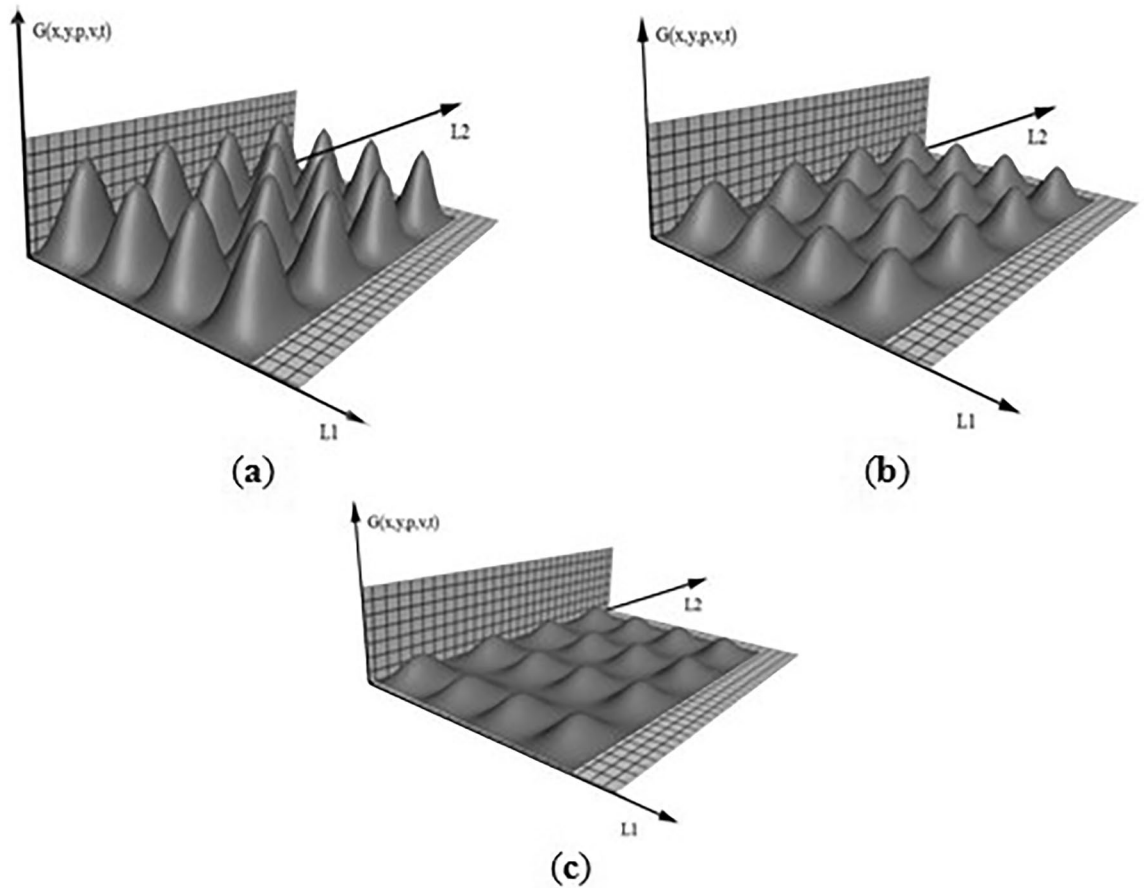


Figure 4. Dynamic change of the temperature field depending on time. (a) before change; (b) cycle change; (c) after change (RAD Studio 11.1 programming environment Delphi <https://www.embarcadero.com/products/rad-studio>).

of unit power. The existing Green's function is one-dimensional. The author obtained a two-dimensional model of the optimal oil production regime.

Thus, it is possible to determine the optimal (smallest) number of heating elements required to maintain a given temperature regime³⁷.

Results

Numerical example. For this, a mathematical model was obtained to determine the places and moments of switching on the heating elements based on the formulated optimality criterion for the two-dimensional case.

$$x = \arcsin \frac{\frac{4}{l_1 l_2} \sum_{k,m=1}^{\infty} \sin\left(\frac{m\pi y}{l_2}\right) \sin\left(\frac{k\pi \rho}{l_1}\right) \sin\left(\frac{m\pi v}{l_2}\right) \exp\left[-a^2 \pi^2 t \left(\frac{k^2}{l_1^2} + \frac{m^2}{l_2^2}\right)\right]}{G(x, y, \rho, v, t)} \left(\frac{l_1}{k\pi}\right); \tag{7}$$

$$y = \arcsin \frac{\frac{4}{l_1 l_2} \sum_{k,m=1}^{\infty} \sin\left(\frac{m\pi x}{l_1}\right) \sin\left(\frac{k\pi \rho}{l_1}\right) \sin\left(\frac{m\pi v}{l_2}\right) \exp\left[-a^2 \pi^2 t \left(\frac{k^2}{l_1^2} + \frac{m^2}{l_2^2}\right)\right]}{G(x, y, \rho, v, t)} \left(\frac{l_2}{m\pi}\right). \tag{8}$$

$$t = \frac{\ln\left(\frac{\frac{4}{l_1 l_2} \sum_{k,m=1}^{\infty} \sin\left(\frac{k\pi x}{l_1}\right) \sin\left(\frac{m\pi y}{l_2}\right) \sin\left(\frac{k\pi \rho}{l_1}\right) \sin\left(\frac{m\pi v}{l_2}\right) \exp\left[-a^2 \pi^2 t \left(\frac{k^2}{l_1^2} + \frac{m^2}{l_2^2}\right)\right]}{G(x, y, \rho, v, t)}\right)}{a^2 \pi^2} \left(\frac{l_1^2}{k^2} + \frac{l_2^2}{m^2}\right). \tag{9}$$

And three-dimensional case

$$x = \frac{l_1}{\pi} \arcsin \frac{\frac{8}{l_1 l_2 l_3} \exp\left[-a^2 \pi^2 t \left(\frac{1}{l_1^2} + \frac{1}{l_2^2} + \frac{1}{l_3^2}\right)\right] \cdot \sin\frac{\pi}{l_2} y \cdot \sin\frac{\pi}{l_3} z \cdot \sum_{i=1}^d \sin\frac{\pi}{l_1} \rho_i \cdot \sin\frac{\pi}{l_2} v_i \cdot \sin\frac{\pi}{l_3} \vartheta_i}{T(x, y, z, t)}.$$

$$y = \frac{l_2}{\pi} \cdot \arcsin \frac{\frac{8}{l_1 l_2 l_3} \exp\left[-a^2 \pi^2 t \left(\frac{1}{l_1^2} + \frac{1}{l_2^2} + \frac{1}{l_3^2}\right)\right] \cdot \sin\frac{\pi}{l_1} x \cdot \sin\frac{\pi}{l_3} z \cdot \sum_{i=1}^d \sin\frac{\pi}{l_1} \rho_i \cdot \sin\frac{\pi}{l_2} v_i \cdot \sin\frac{\pi}{l_3} \vartheta_i}{T(x, y, z, t)}. \tag{10}$$

$$z = \frac{l_3}{\pi} \cdot \arcsin \frac{\frac{8}{l_1 l_2 l_3} \exp\left[-a^2 \pi^2 t \left(\frac{1}{l_1^2} + \frac{1}{l_2^2} + \frac{1}{l_3^2}\right)\right] \cdot \sin\frac{\pi}{l_1} x \cdot \sin\frac{\pi}{l_2} y \cdot \sum_{i=1}^d \sin\frac{\pi}{l_1} \rho_i \cdot \sin\frac{\pi}{l_2} v_i \cdot \sin\frac{\pi}{l_3} \vartheta_i}{T(x, y, z, t)}.$$

On the basis of these equations, a large number of computer and natural experiments were carried out, which showed the occurrence of thermal deformation of the tubing. To analyze thermal deformation, we will analyze the mathematical model.

$$\frac{dT_1(x, r, \Theta, \tau)}{d\tau} = a_1 \cdot \left(\frac{d^2 T_1(x, r, \Theta, \tau)}{dr^2} + \frac{1}{r} \cdot \frac{dT_1(x, r, \Theta, \tau)}{dr} + \frac{d^2 T_1(x, r, \Theta, \tau)}{dx^2} + \frac{1}{r} \cdot \frac{d^2 T_1(x, r, \Theta, \tau)}{d\Theta^2} \right), \tag{11}$$

$$0 < x < L, R_2 < r < R_1, 0 < \Theta < 360^\circ. \tag{12}$$

Temperature field of oil flow

$$\frac{dT_2(x, r, \Theta, \tau)}{d\tau} = a_2 \cdot \left(\frac{d^2 T_2(x, r, \Theta, \tau)}{dr^2} + \frac{1}{r} \cdot \frac{dT_2(x, r, \Theta, \tau)}{dr} + \frac{d^2 T_2(x, r, \Theta, \tau)}{dx^2} + \frac{1}{r} \cdot \frac{d^2 T_2(x, r, \Theta, \tau)}{d\Theta^2} \right), \tag{13}$$

$$0 < x < L, 0 < r < R_2, 0 < \Theta < 360^\circ. \tag{14}$$

Boundary conditions for the phase variable T_1

$$\lambda_1 \frac{dT_1(x, R_1, \Theta, \tau)}{dr} = \lambda_B \frac{dT_B(x, R_1, \Theta, \tau)}{dr}, \tag{15}$$

$$T_1(x, R_1, \Theta, \tau) = T_B(x, R_1, \Theta, \tau); 0 < x < L, 0 < \Theta < 360^\circ. \tag{16}$$

Boundary conditions for the phase variable T_2

$$\lambda_1 \frac{dT_1(x, R_2, \Theta, \tau)}{dr} = \lambda_2 \frac{dT_2(x, R_2, \Theta, \tau)}{dr}; \tag{17}$$

$$T_1(x, R_2, \Theta, \tau) = T_2(x, R_2, \Theta, \tau); \tag{18}$$

$$0 < x < L, 0 < \Theta < 360^\circ \tag{19}$$

End faces of the object

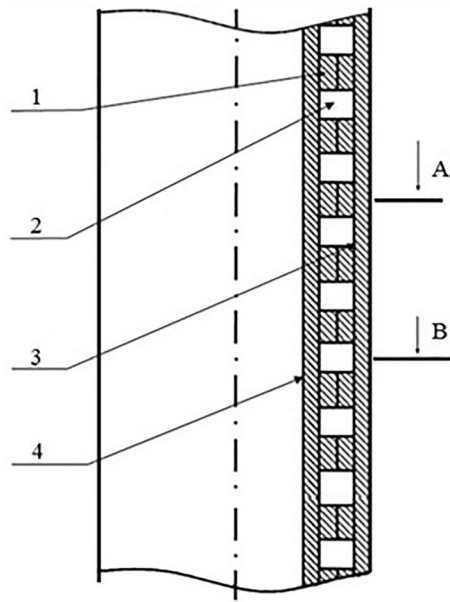


Figure 5. Scheme of tubing with impulse sectional heaters.

$$\begin{aligned} T_1(0, r, \Theta, \tau) = T_1(L, r, \Theta, \tau) = 0; R_2 < r < R_1; \\ T_2(0, r, \Theta, \tau) = T_2(L, r, \Theta, \tau) = 0; 0 < r < R_2; \end{aligned} \tag{20}$$

Then, the final equation for estimating the thermal deformation of the tubing wellbore has the form

$$f = \sum_{j=1}^N \text{arctg}((\Delta x_j - \Delta x)/(2R_3)). \tag{21}$$

Thermodynamic properties. The final step in the assessment of the regulatory system is the determination of sustainability. It should be noted that the control system is non-linear, and therefore there are no methods for assessing stability. We adapt the Nyquist stability criterion for an impulsive distributed system. To do this, we obtain the transfer function of an open-loop control system, which is written as follows.

$$\begin{aligned} W_P^*(G_{\eta,\gamma}, s) = (1 - \exp(-st)) \cdot \frac{1}{s} \cdot \frac{1}{t} \cdot \sum_{r=-\infty}^{r=\infty} \left(\left(E_1 \cdot \left[\frac{n_1 - 1}{n_1} + \frac{1}{n_1} \cdot G_{\eta,\gamma} \right] + E_4 \cdot \left[\frac{n_4 - 1}{n_4} + \frac{1}{n_4} \cdot G_{\eta,\gamma} \right] \right. \right. \\ \left. \left. \cdot \frac{1}{s} + E_2 \cdot \left[\frac{n_2 - 1}{n_2} + \frac{1}{n_2} \cdot G_{\eta,\gamma} \right] \cdot s \right) \cdot \frac{\exp(\beta(G_{\eta,\gamma} \cdot z^*)) + \exp(-\beta(G_{\eta,\gamma} \cdot z^*))}{\lambda \cdot \beta(G_{\eta,\gamma}) \cdot (\exp(\beta(G_{\eta,\gamma}) \cdot z_L) - \exp(-\beta(G_{\eta,\gamma}) \cdot z_L))} \right), \\ \beta = \left(\frac{s + jr\omega_u}{a} + G_{\eta,\gamma} \right)^{1/2}, (\eta, \gamma = \overline{1, \infty}) \end{aligned} \tag{22}$$

By passing from an infinite number of circles of unit radius, we obtain the hodograph of a spatially distributed impulse control system, Fig. 5.

Sectional heating elements are controlled by a programmable unit, Fig. 5, consisting of four arithmetic logic units.

These logical elements are connected in parallel, which ensures a high speed of generating command signals. Figure 6 shows the main control circuit with control signal output indicators.

In addition, on the basis of the methods obtained, a number of thermal drills were obtained and tested on an industrial scale, performing various specific tasks of exploration and thermal drilling in the conditions of the Arctic zone. Experimental studies were carried out on an electron microscope in various modes, demonstrating uniform heating of the metal. The results of the experiment confirm the absence of destruction of the metal structure caused by pulsed heating.

Discussions

As part of the study, a tubing with impulse sectional heaters was developed, consisting of external and internal casings and impulse-type heating elements installed between them, separated by bulkheads with a current-carrying channel inside. The principle of operation of this device can be divided into two modes: static and dynamic.

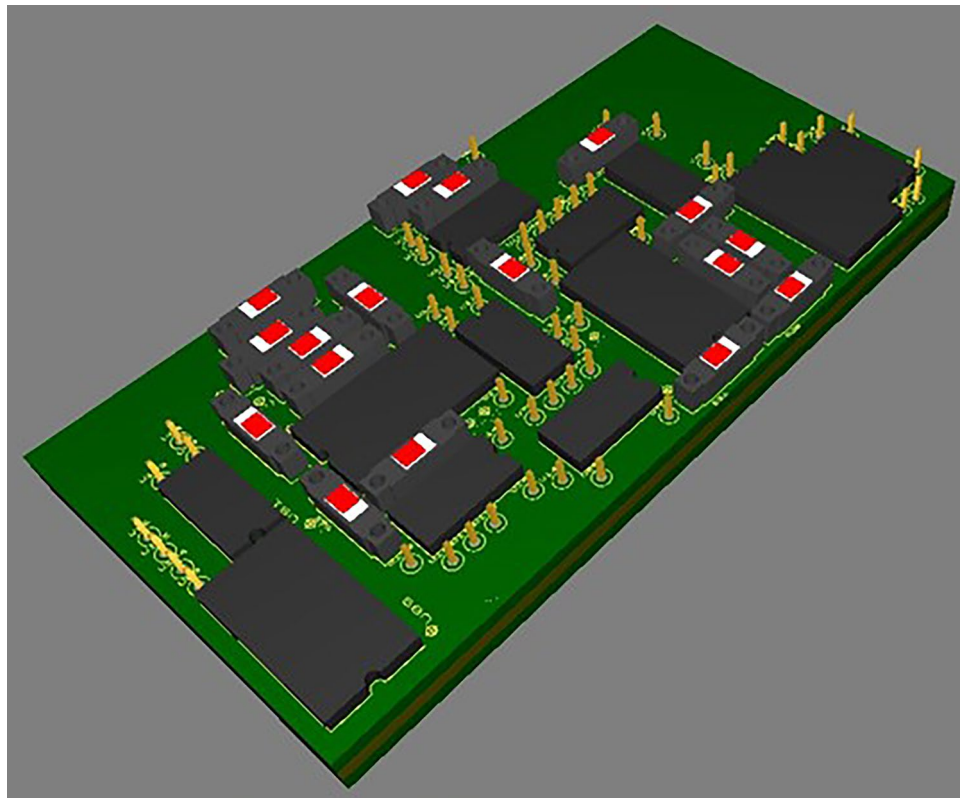


Figure 6. Layout model of parallel computing unit (top view). (Multisim <https://www.ni.com/shop/electronic-test-instrumentation/application-software-for-electronic-test-and-instrumentation-category/what-is-multisim.html>).

In static mode, the tubing string with impulse sectional heaters is not connected to the power supply. In this mode, the electric current is not supplied to the heaters, the temperature field is not formed. All structural elements located on a metal sleeve are at rest at ambient temperature. Oil rising through such a tubing cools, its rheological properties change, it becomes more viscous. Asphalt, resin and paraffin deposits begin to form on the tubing walls (Supplementary 1 Video). Asphalt-resin-paraffin deposits increase over time, which leads to a complete overlap of the column.

In dynamic mode, the tubing string is connected to the power supply network. In this mode, a pulsed current is applied to the heating elements and the temperature rises. Over time, the heating of the metal sleeve, the bulkhead and the entire structure as a whole begins. The tubing is heated above the paraffin temperature. Thus, asphalt-resin-paraffin deposits do not form on the tubing walls. Oil continues to rise along the tubing.

When compared with constant heating, which forms a temperature field, energy costs are reduced up to 4...6 times. It is important to note that the number and extent of installation of such heaters is not limited (Supplementary 2).

The methods presented above made it possible to obtain the optimal number of heating elements based on a given temperature regime. The production process at each field is unique and requires a specific approach to it, so there is no need to create a tubing block for each field individually. Thus, it is expedient to create a unified tubing that provides any technological regime. In this regard, in the presented technical device, the heating elements are located equidistantly at the minimum possible distance, without prejudice to the design features. The developed tubing is suitable for the extraction of highly paraffinic oil from any field.

To prevent paraffin formation and clogging of tubing in the field under consideration, installations for supplying a hydrate formation inhibitor are used, Fig. 7. The installation includes:

- consumable capacity ($V = 5 \text{ m}^3$);
- consumable capacity (Apparatus 1–50-2400, $V = 50 \text{ m}^3$);
- technological block for inhibitor supply (pumping blocks);
- dosing pumps.

The hydrate formation inhibitor is supplied to the wells using dosing pumps from pre-filled containers $V = 5 \text{ m}^3$ or $V = 50 \text{ m}^3$.

After the implementation of the developed automation scheme, the technological process will be carried out as follows. All elements that ensure the injection of the inhibitor, both into the tubing itself and into the main pipeline, are removed from the automation scheme. The extracted oil will have a higher temperature, which

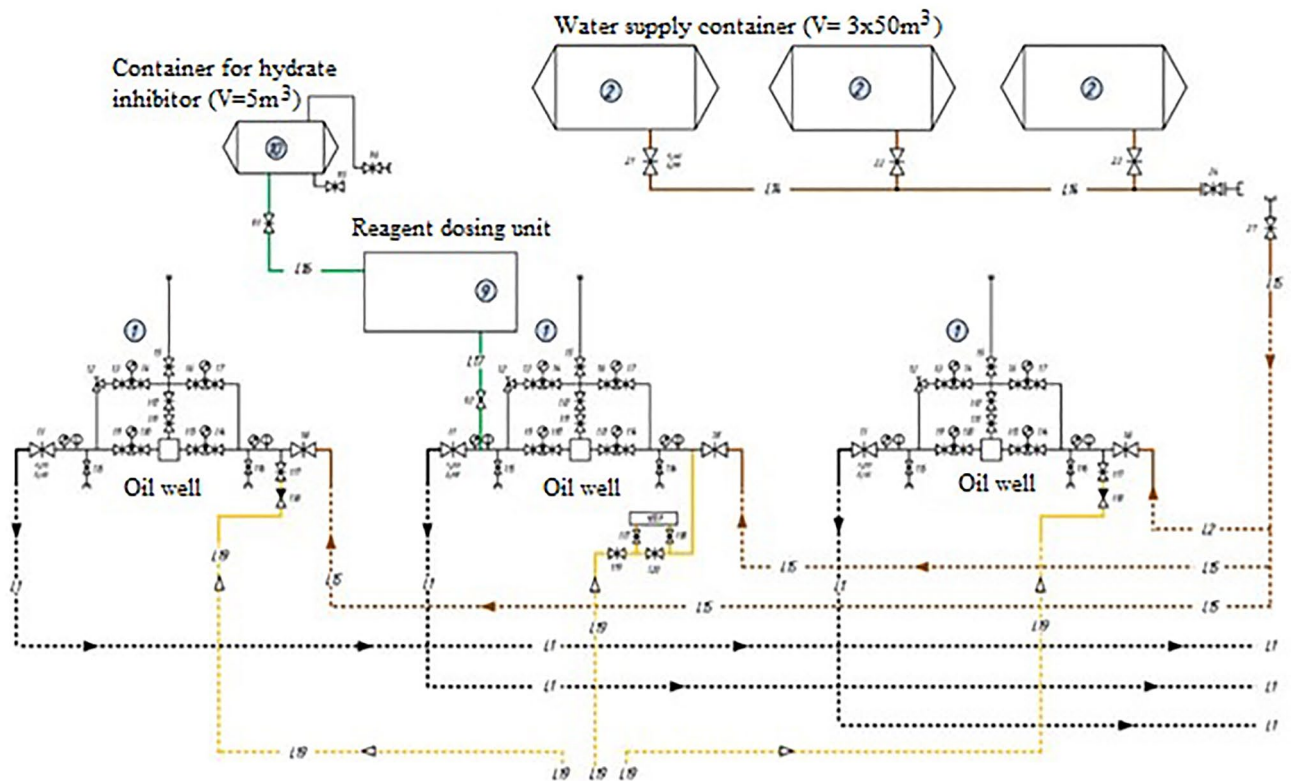


Figure 7. The existing scheme of automation of the technological process.

will ensure that it does not need to be further diluted. This will have the economic effect of saving money on inhibitor storage tank rental and logistics costs. The elements of heating the heating cable are removed, in view of its exclusion from the circuit. At the same time, the existing automation scheme is being retrofitted with a controller for controlling pulsed sectional heaters, and power supply loops are being installed. The proposed automation scheme is shown in Fig. 8.

This Figure shows the installation location of the control unit. The connection points of the supply loops are shown schematically, this is mainly due to the geographical features of the relief and the availability of power supply points.

Conclusions

The paper analyzes in detail the existing scheme for automating the technological process of oil production from fields with a high content of paraffin. The technological process of cleaning downhole equipment from Asphalt-resinous and paraffin deposits is considered. The cause-and-effect relationships of deposit formation were also considered. On the basis of the work done, conclusions were drawn about the effectiveness of the use of thermal control methods, but also their high cost. Further, mathematically calculated, and then implemented in the form of technical devices, elements of automated process control systems that provide a more effective technology for combating and preventing the formation of Asphalt-resinous and paraffin deposits. The main tasks implemented in the framework of the study include:

1. A analysis of the scheme of the technological process for the production of high-paraffin oil from fields with a low flow rate was carried out, within the framework of which: research of temperature fields and synthesis of pulsed control of the temperature field based on the Green's function of the wall of a multi-section heater were carried out, taking into account the spatial configuration of the pump-compressor pipes; a mathematical model was built and a system for diagnosing temperature deformation of a tubing due to heat exchange processes was synthesized; developed a method for the optimal location of heating elements on the tubing wall, based on the specified measurement error; a scheme for automating the technological process of extraction of high-paraffin oil from marginal deposits was developed. Also, specialized software has been developed that implements the functioning of the technical part of the presented study. A method has been developed for determining absolute stability based on the Nyquist criterion for impulsive distributed systems for which there is a fundamental solution in the form of a Green's function. Substantiation and development, based on a mathematical model, of recommendations for the smallest number of heating elements integrated into the structure of oilfield tubing.
2. As part of the study, a number of devices were developed that ensure the automation of the technological process, namely: a tubing with impulse sectional heaters was developed; a number of topologies of integrated

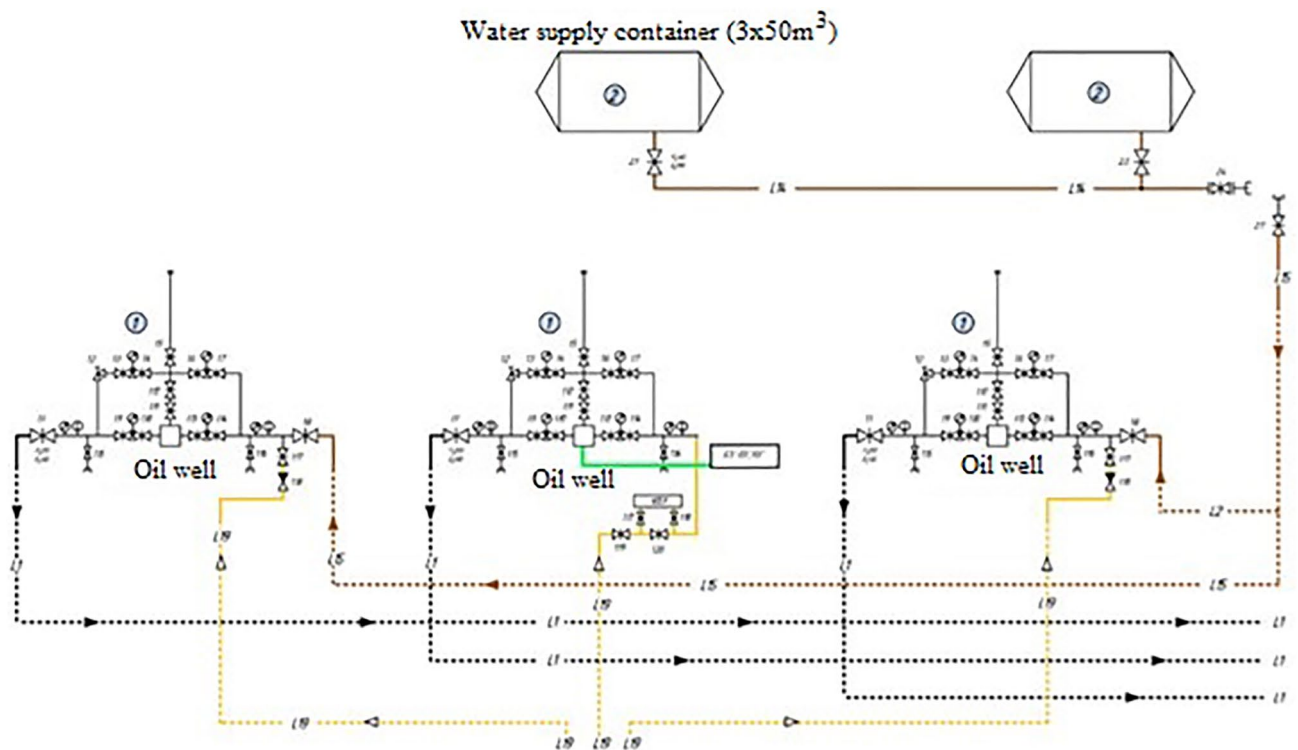


Figure 8. Proposed automation scheme.

circuits have been developed to ensure the operation of tubing with pulsed sectional heaters; a number of heating elements with impulse sectional heaters has been developed.

3. Specialized software has been developed for modeling and functioning of the schemes of the developed technological process.

Thus, all the tasks set in this study were completed in full. The resulting technical devices have passed pilot tests.

Data availability

All data generated or analysed during this study are included in this published article and its supplementary information files. Request for more details to the corresponding author.

Received: 22 April 2022; Accepted: 4 October 2022

Published online: 01 November 2022

References

1. Lira-Galeana, C. & Hammami, A. Chapter 21 Wax precipitation from petroleum fluids: A review. *Dev. Pet. Sci. Part B* **40**, 557–608. [https://doi.org/10.1016/S0376-7361\(09\)70292-4](https://doi.org/10.1016/S0376-7361(09)70292-4) (2000).
2. Girma, T. C., Sulaiman, S. A., Japper-Jaafar, A., Wan Ahmad, W. A. K. & Mokhtar, M. M. M. Gas void formation in statically cooled waxy crude oil. *Int. J. Ther. Sci.* **86**, 41–47. <https://doi.org/10.1016/j.ijthermalsci.2014.06.034> (2014).
3. Li, W. *et al.* A theoretical model for predicting the wax breaking force during pipeline pigging. *J. Pet. Sci. Eng.* **169**, 654–662. <https://doi.org/10.1016/j.petrol.2018.05.078> (2018).
4. Li, W. *et al.* Estimating the wax breaking force and wax removal efficiency of cup pig using orthogonal cutting and slip-line field theory. *Fuel* **236**, 1529–1539. <https://doi.org/10.1016/j.fuel.2018.09.132> (2019).
5. Nikolaev, A. K., Dokoukin, V. P., Lykov, Y. V. & Fetisov, V. G. Research of processes of heat exchange in horizontal pipeline. *IOP Conf. Ser. Mater. Sci. Eng.* **327**, 032041. <https://doi.org/10.1088/1757-899X/327/3/032041> (2018).
6. Fetisov, V., Tcvetkov, P. & Müller, J. Tariff approach to regulation of the European gas transportation system: Case of Nord Stream. *Energy Rep.* **7**(Supplement 6), 413–425. <https://doi.org/10.1016/j.egyrs.2021.08.023> (2021).
7. Litvinenko, V. S., & Dvoynikov, M. V. Monitoring and control of the drilling string and bottomhole motor work dynamics. In *Balkema Topical Issues of Rational Use of Natural Resources*. CRC Press, Leiden, The Netherlands (2019), Volume 1, pp. 804–809. <https://doi.org/10.1201/9781003014638-42>.
8. Litvinenko, V. S. Technological Progress Having Impact on Coal Demand Growth. In *XVIII International Coal Preparation Congress*; Springer: Cham, Switzerland, (2016); pp.1–8. https://doi.org/10.1007/978-3-319-40943-6_1.
9. Pashkevich, N. V., Tarabarina, T. A. & Golovina, E. Problems of reflecting information on subsoil assets in international financial reporting standards. *Acad. Strateg. Manag. J.* **17**, 1–4 (2018).
10. Girma, T. C., Sulaiman, S. A. & Japper-Jaafar, A. Flow start-up and transportation of waxy crude oil in pipelines—A review. *J. Non-Newton. Fluid Mech.* **251**, 69–87. <https://doi.org/10.1016/j.jnnfm.2017.11.008> (2018).
11. Li, N., Mao, G. L., Shi, X. Z., Tian, S. W. & Liu, Y. Advances in the research of polymeric pour point depressant for waxy crude oil. *J. Dispers. Sci. Technol.* **39**, 1165–1171. <https://doi.org/10.1080/01932691.2017.1385484> (2018).

12. Elbanna, S. A., Abd El Rhman, A. M., Al-Hussaini, A. S. & Salah, A. K. Synthesis, characterization, and performance evaluation of novel terpolymers as pour point depressors and paraffin inhibitors for Egyptian waxy crude oil. *Pet. Sci. Technol.* **40**, 2263–2283. <https://doi.org/10.1080/10916466.2022.2041660> (2022).
13. Paulya, J., Daridona, J. L., Sansot, J. M. & Coutinho, J. A. P. The pressure effect on the wax formation in diesel fuel. *Fuel* **82**, 595–601. [https://doi.org/10.1016/S0016-2361\(02\)00316-2](https://doi.org/10.1016/S0016-2361(02)00316-2) (2003).
14. Ashmawy, A. M. *et al.* Allyl ester-based liquid crystal flow improvers for waxy crude oils. *J. Dispers. Sci. Technol.* **42**, 2199–2209. <https://doi.org/10.1080/01932691.2021.1981367> (2021).
15. Huang, Z., Xin, Pu., Jiawen, Hu., Jin, Gu. & Liu, J. Study on structure control and pour point depression mechanism of comb-type copolymers. *Pet. Sci. Technol.* **39**, 777–794. <https://doi.org/10.1080/10916466.2021.1927078> (2021).
16. Eke, W. I., Achugasim, O., Ajenka, J. & Akaranta, O. Glycerol-modified cashew nut shell liquid as eco-friendly flow improvers for waxy crude oil. *Pet. Sci. Technol.* **39**, 101–114. <https://doi.org/10.1080/10916466.2020.1849284> (2021).
17. Ahmed, S. M., Khidr, T. T. & Ali, E. S. Preparation and evaluation of polymeric additives based on poly(styrene-co-acrylic acid) as pour point depressant for crude oil. *J. Dispers. Sci. Technol.* **33**, 1–8. <https://doi.org/10.1080/01932691.2021.1878038> (2021).
18. Todt, S., & Deo, M. Experimental and modeling studies of wax deposition in crude-oil-carrying pipelines. Paper presented at the Offshore Technology Conference, Houston, TX, USA, 1–4 May (2006). <https://doi.org/10.4043/18368-MS>.
19. Smith, P. B., & Ramsden, R. M. J. The prediction of oil gelation in submarine pipelines and the pressure required for restarting flow. Paper presented at the SPE European Petroleum Conference, London, UK, 24–27 October (1978). <https://doi.org/10.2118/8071-MS>.
20. Huang, H. *et al.* The influence of nanocomposite pour point depressant on the crystallization of waxy oil. *Fuel* **221**, 257–268. <https://doi.org/10.1016/j.fuel.2018.01.040> (2018).
21. Yang, F. *et al.* Hydrophilic nanoparticles facilitate wax inhibition. *Energy Fuels* **29**, 1368–1374. <https://doi.org/10.1021/ef502392g> (2015).
22. Paso, K., Silset, A. & Sørland, G. Characterization of the formation, flowability, and resolution of Brazilian crude oil emulsions. *Energy Fuels* **23**, 471–480. <https://doi.org/10.1021/ef800585s> (2009).
23. Kané, M., Djabourov, M., Volle, J.-L., Lechaire, J.-P. & Frebourg, G. Morphology of paraffin crystals in waxy crude oils cooled in quiescent conditions and under flow. *Fuel* **82**, 127–135. [https://doi.org/10.1016/S0016-2361\(02\)00222-3](https://doi.org/10.1016/S0016-2361(02)00222-3) (2003).
24. Kané, M., Djabourov, M. & Volle, J.-L. Rheology and structure of waxy crude oils in quiescent and under shearing conditions. *Fuel* **83**, 1591–1605. <https://doi.org/10.1016/j.fuel.2004.01.017> (2004).
25. Chi, Y., Daraboina, N. & Sarica, C. Investigation of inhibitors efficacy in wax deposition mitigation using a laboratory scale flow loop. *AIChE J.* **62**, 4131–4139. <https://doi.org/10.1002/aic.15307> (2016).
26. Chi, Y., Daraboina, N. & Sarica, C. Effect of the flow field on the wax deposition and performance of wax inhibitors: Cold finger and flow loop testing. *Energy Fuels* **31**, 4915–4924. <https://doi.org/10.1021/acs.energyfuels.7b00253> (2017).
27. Martínez-Palou, R. *et al.* Transportation of heavy and extra-heavy crude oil by pipeline: A review. *J. Pet. Sci. Eng.* **75**, 274–282. <https://doi.org/10.1016/j.petrol.2010.11.020> (2011).
28. Nurgalieva, K. S., Saychenko, L. A. & Riazi, M. Improving the efficiency of oil and gas wells complicated by the formation of Asphalt-Resin-Paraffin deposits. *Energies* **14**, 6673. <https://doi.org/10.3390/en14206673> (2021).
29. Afdhol, M. K., Abdurrahman, M., Hidayat, F., Chong, F. K. & Mohd Zaid, H. F. Review of solvents based on biomass for mitigation of wax paraffin in Indonesian oilfield. *Appl. Sci.* **9**, 5499. <https://doi.org/10.3390/app9245499> (2019).
30. Sayani, J. K. S., Pedapati, S. R. & Lal, B. Phase behavior study on gas hydrates formation in gas dominant multiphase pipelines with crude oil and high CO₂ mixed gas. *Sci. Rep.* **10**, 14748. <https://doi.org/10.1038/s41598-020-71509-6> (2020).
31. El-Dalatony, M. M. *et al.* Occurrence and characterization of paraffin wax formed in developing wells and pipelines. *Energies* **12**, 967. <https://doi.org/10.3390/en12060967> (2019).
32. Zhang, H. *et al.* Probabilistic analysis of water-sealed performance in underground oil storage considering spatial variability of hydraulic conductivity. *Sci. Rep.* **12**, 13782. <https://doi.org/10.1038/s41598-022-16960-3> (2022).
33. Fethiza Tedjani, C. *et al.* Crude oil sensing using carbon nano structures synthesized from *Phoenix Dactylifera* L. cellulose. *Sci. Rep.* **9**, 17806. <https://doi.org/10.1038/s41598-019-54417-2> (2019).
34. Mizuhara, Jo. *et al.* Evaluation of asphaltene adsorption free energy at the oil-water interface: Role of heteroatoms. *Energy Fuels* **34**(5), 5267–5280. <https://doi.org/10.1021/acs.energyfuels.9b03864> (2020).
35. Dolgi, I. E. Methods to enhance oil recovery in the process of complex field development of the Yarega oil and titanium deposit. *J. Min. Inst.* **231**, 263. <https://doi.org/10.25515/pmi.2018.3.263> (2018).
36. Fazeli, M. *et al.* Experimental analyzing the effect of n-heptane concentration and angular frequency on the viscoelastic behavior of crude oil containing asphaltene. *Sci. Rep.* **12**, 3965. <https://doi.org/10.1038/s41598-022-07912-y> (2022).
37. Psoni, H. & Bharambe, D. P. Energy & fuels performance-based designing of wax crystal growth inhibitors. *Energy Fuels* **22**, 3930–3938. <https://doi.org/10.1021/ef8002763> (2008).
38. Molchanov, A. A. & Ageev, P. Implementation of new technology is a reliable method of extracting reserves remaining in hydrocarbon deposits. *J. Min. Inst.* **227**, 530. <https://doi.org/10.25515/pmi.2017.5.530> (2017).
39. Rogachev, M. K., Mukhametshin, V. V. & Kuleshova, L. S. Improving the efficiency of using resource base of liquid hydrocarbons in Jurassic deposits of Western Siberia. *J. Min. Inst.* **240**, 711. <https://doi.org/10.31897/pmi.2019.6.711> (2019).
40. Yang, F., Zhao, Y., Sjöblom, J., Li, C. & Paso, K. G. Polymeric wax inhibitors and pour point depressants for waxy crude oils: A critical review. *J. Dispers. Sci. Technol.* **36**, 213–225. <https://doi.org/10.1080/01932691.2014.901917> (2015).
41. Xie, J. *et al.* Cold damage from wax deposition in a shallow, low-temperature, and high-wax reservoir in Changchunling Oilfield. *Sci. Rep.* **10**, 14223. <https://doi.org/10.1038/s41598-020-71065-z> (2020).
42. de Lara, L. S., Voltatoni, T., Rodrigues, M. C., Miranda, C. R. & Brochsztain, S. Potential applications of cyclodextrins in enhanced oil recovery. *Colloids Surf. A Physicochem. Eng. Asp.* **469**, 42–50. <https://doi.org/10.1016/j.colsurfa.2014.12.045> (2015).
43. Lu, T. *et al.* Flow behavior of N₂ huff and puff process for enhanced oil recovery in tight oil reservoirs. *Sci. Rep.* **7**, 15695. <https://doi.org/10.1038/s41598-017-15913-5> (2017).
44. Karpikov, A. V., Aliev, R. I. & Babyr, N. V. An analysis of the effectiveness of hydraulic fracturing at YS1 of the Northern field. *IOP Conf. Ser. Mater. Sci. Eng.* **952**, 012036. <https://doi.org/10.1088/1757-899X/952/1/012036> (2020).
45. Kazanin, O. I., Sidorenko, A. A. & Sirenko, Y. G. Numerical study of the air-gas dynamic processes when working out the Mosshny seam with longwall faces. *ARPN J. Eng. Appl. Sci.* **13**, 1534–1538 (2018).
46. Yang, F., Li, C., Li, C. & Wang, D. Scaling of structural characteristics of gelled model waxy oils. *Energy Fuels* **27**, 3718–3724. <https://doi.org/10.1021/ef400554v> (2013).
47. Demirbas, A., Alidrisi, H. & Balubaid, M. A. API gravity, sulfur content, and desulfurization of crude oil. *Pet. Sci. Technol.* **33**, 93–101. <https://doi.org/10.1080/10916466.2014.950383> (2015).
48. Demirbas, A. Deposition and flocculation of asphaltenes from crude oils. *Pet. Sci. Technol.* **34**, 6–11. <https://doi.org/10.1080/10916466.2015.1115875> (2016).
49. Ganeeva, Y. M., Yusupova, T. N. & Romanov, G. V. Waxes in asphaltenes of crude oils and wax deposits. *Pet. Sci.* **13**, 737–745. <https://doi.org/10.1007/s12182-016-0111-8> (2016).
50. Japper-Jaafar, A., Bhaskoro, P. T. & Mior, Z. S. A new perspective on the measurements of wax appearance temperature: Comparison between DSC, thermomicroscopy and rheometry and the cooling rate effects. *J. Pet. Sci. Eng.* **147**, 672–681. <https://doi.org/10.1016/j.petrol.2016.09.041> (2016).

51. Nermen, H., Fathi, M., Soliman, S., El Maghraby, H. & Moustfa, Y. M. Thermal conductivity enhancement of treated petroleum waxes, as phase change material, by α nano alumina: Energy storage. *Renew. Sustain. Energy Rev.* **70**, 1052–1058. <https://doi.org/10.1016/j.rser.2016.12.009> (2017).
52. Olajire, A. A. Review of wax deposition in subsea oil pipeline systems and mitigation technologies in the petroleum industry. *Chem. Eng. J. Adv.* **6**, 100104. <https://doi.org/10.1016/j.cej.2021.100104> (2021).
53. Ilyushin, A. N., Shilkina, I. D. & Afanasev, P. M. Design of automated control system supporting temperature field in. *Int. Multi-Conf. Ind. Eng. Mod. Technol.* **2019**, 1–4. <https://doi.org/10.1109/FarEastCon.2019.8934041> (2019).
54. Pershin, I. M., Kukharova, T. V. & Tsapleva, V. V. Designing of distributed systems of hydrolithosphere processes parameters control for the efficient extraction of hydromineral raw materials. *J. Phys. Conf. Ser.* <https://doi.org/10.1088/1742-6596/1728/1/012017> (2021).
55. Martirosyan, A. V., Martirosyan, K. V. Quality improvement information technology for mineral water field's control. In *Proceedings of the 2016 IEEE Conference on Quality Management, Transport and Information Security, Nalchik, Russia*, 4–11 October (2016), pp. 147–151. <https://doi.org/10.1109/ITMQIS.2016.7751925>.
56. Ilyushin, A. N., Kovalev, D. A., Afanasev, P. M. Development of information measuring complex of distributed pulse control system. In *Proceedings of the International Multi-Conference on Industrial Engineering and Modern Technologies, Vladivostok, Russia*, 1–4 October (2019), pp. 1–5. <https://doi.org/10.1109/FarEastCon.2019.8934173>.
57. Nejad, S. A. T. & Khodapanah, E. Application of Gaussian quadrature method to characterize heavy end of hydrocarbon fluids for modeling wax deposition. *Appl. Math. Model.* **35**, 109–122. <https://doi.org/10.1016/j.apm.2010.05.010> (2011).

Acknowledgements

This research was a personal initiative of the authors who took part in the experiments. Thank you to all participants in the research.

Author contributions

Y.V.I. contributed to the conception of the study, performed the experiment, provided the original data, wrote the manuscript; V.F. contributed significantly to analysis and manuscript preparation, performed the data analyses and edited the manuscript; Y.V.I. and V.F. the analysis with constructive discussions. Reviewed both the experiments and drafts of the paper, and approved the final draft. All authors critically reviewed and approved the manuscript.

Competing interests

The authors declare no competing interests.

Additional information

Supplementary Information The online version contains supplementary material available at <https://doi.org/10.1038/s41598-022-21778-0>.

Correspondence and requests for materials should be addressed to Y.V.I. or V.F.

Reprints and permissions information is available at www.nature.com/reprints.

Publisher's note Springer Nature remains neutral with regard to jurisdictional claims in published maps and institutional affiliations.



Open Access This article is licensed under a Creative Commons Attribution 4.0 International License, which permits use, sharing, adaptation, distribution and reproduction in any medium or format, as long as you give appropriate credit to the original author(s) and the source, provide a link to the Creative Commons licence, and indicate if changes were made. The images or other third party material in this article are included in the article's Creative Commons licence, unless indicated otherwise in a credit line to the material. If material is not included in the article's Creative Commons licence and your intended use is not permitted by statutory regulation or exceeds the permitted use, you will need to obtain permission directly from the copyright holder. To view a copy of this licence, visit <http://creativecommons.org/licenses/by/4.0/>.

© The Author(s) 2022